Gravitational self-interactions of cosmic strings

Jean M. Quashnock*
Joseph Henry Laboratories, Princeton University, Princeton, New Jersey 08544

David N. Spergel
Department of Astrophysical Sciences, Princeton University, Princeton, New Jersey 08544

(Received 16 April 1990)

We study the gravitational back reaction of local cosmic-string loops as they shrink due to gravitational radiation. We chart the evolution of the shape and radiation rate of the loops. Cusps survive gravitational back reaction, but are weakened. Asymmetric string trajectories radiate momentum and hence undergo a rocket effect, but the effect is not very significant. Typically, a string loop's center-of-mass velocity is changed by $\Delta v \sim 0.1c$. Trajectories that have few modes and that are non-self-intersecting remain so almost until the end of the string's lifetime. We also study highly kinky loops. Small kinks decay very quickly, the decay time for a kink of size l being given by $t(l)_{\text{decay}} \sim (\Gamma_{\text{kink}} G\mu)^{-1} l$, where $\Gamma_{\text{kink}} \sim 50$. We argue that this limits the smallest relevant structures on long strings in networks to a fraction $(\Gamma_{\text{kink}} G\mu)$ of the size of the horizon, and that this will also set the scale for loops produced off a network. This, coupled with results from string network simulations and millisecond-pulsar constraints, limits the string tension to $G\mu < 2 \times 10^{-5}$. This is far from ruling out the cosmic-string scenario of galaxy formation.

I. INTRODUCTION

In the last several years there has been much interest in cosmic strings and their astrophysical consequences, particularly in the cosmic-string scenario of galaxy formation. The long string evolution is described quite well by the "one-scale" scaling solution,[1] with ξ growing as the horizon size $2t$. However, in some of the simulations,[2] neither the size of the small loops chopped off the network nor the small-scale structure on the long strings appear to be scaling with the horizon size. There is lively debate[3] on the amount, generation, and scale of structure on the long strings. Several numerical simulations[4] show that the long strings comprising the network develop significant structure on scales much smaller than the scale length of the network, and that the size of the stable loops produced by the networks is determined by this small-scale structure. These simulations show no lower limit to small-scale structure; indeed, the structure on the strings is seen down to the resolution of the numerical simulations.

Kinks, which are discontinuities in the tangent vector of the string, are inevitably formed when strings intersect.[5] Thus, as the network is evolved and strings intersect and form loops, kinks accumulate on the long strings, and their structure becomes more and more crinkly. Correspondingly, the size of loops produced by the network shrinks relative to the horizon.

It is important to know what this size is, because the amount and spectrum of the gravitational radiation emitted by the loops is a direct function of their size relative to the horizon.[6] This also means that the constraints from millisecond-pulsar measurements,[7] in particular, the limits placed on the strong tension $G\mu$, depend on a detailed understanding of small-scale structure on cosmic strings.

In the next section, we present our formalism for treating string back reactions. We then describe the numerical algorithm used to compute cosmic-string evolution. In the penultimate section, we discuss the effect of gravitational backreaction on the evolution of cosmic strings. The last section contains the conclusions.

II. THE GRAVITATIONAL BACK-REACTION PROBLEM

We consider the problem of a local cosmic string interacting with its own gravitational field. This problem is the *gravitational back-reaction problem,* simply because the cosmic string is moving in its own gravitational field. The field at a given point on the string (*field point*) is the sum of contributions from points all along the string (*source points*). Of particular interest is the contribution from the field point itself. This is the self-interaction, arising from a point on the string that instantaneously interacts with itself.

As with all back-reaction problems, the possibility of divergences always looms large. These divergences arise when the self-interaction becomes infinite as the source point approaches the field point. The most famous example is the classical electron. Dirac[8] solved the problem of an electron moving in its own electromagnetic field by renormalizing its mass, thereby absorbing the divergent self-interaction term. The leftover finite term is the Dirac-Lorentz back-reaction force, slowing the electron down as it accelerates and radiates. The global string also suffers from infinite back reaction because of the nature of its self-interaction. Dabholkar and Quashknock[9] removed this divergence by renormalizing the string mass per unit length. After the renormalization, there is again a finite leftover piece in the equation of motion, which is simply the back-reaction force.

The gravitational self-interaction of a cosmic string, however, is divergence-free: all the relevant physical quantities are finite and well defined. In Appendix A, the back reaction is treated analytically. Here, we offer a physical argument for the divergence-free nature of cosmic-string gravitational self-interactions. Consider the motion of a point on the string. There, we can transform to coordinates that are locally moving and accelerating with that point. Locally, this reduces the metric to the Minkowski one and sets to zero its first derivatives (the Christoffel connection). By the equivalence principle of general relativity, in such a coordinate system we cannot speak of any gravitational force at all, at least at the point in question. The self-interaction of a point that is instantaneously at rest and nonaccelerating must be zero. Other points nearby will be moving relative to this point, but the tidal interactions between those source points and the field point will be finite. With the gravitational back-reaction problem for cosmic strings, there are no divergences. There is the caveat of cusps, however, since they instantaneously move at the speed of light—there is no rest frame for them and the above argument does not apply. In this case, there one obtains a coordinate divergence, namely, the back-reaction force per coordinate interval diverges. But the integrated force, energy loss, and radiation around the cusp is finite, and so is any other physically measurable quantity.

We now describe the mathematical formalism needed to address these questions, and the above assertions shall be demonstrated quantitatively. Also, recently, a unified treatment of the issue of divergences in several sorts of classical radiating strings has been given in Ref. 10. The same conclusion has been reached as to the divergence-free nature of the gravitational back-reaction problem.

III. THE FORMALISM

Consider a closed string moving in space-time $x^\mu(\sigma,\tau)$. For an infinitely thin string, the only relevant quantity describing the world sheet of the string is its area, and hence the action for the string is given by the Nambu action[11]

$$S=-\mu\int d\sigma\, d\tau[(g_{\alpha\beta}\partial_\tau x^\alpha\partial_\sigma x^\beta)^2 -(g_{\alpha\beta}\partial_\tau x^\alpha\partial_\tau x^\beta)(g_{\gamma\delta}\partial_\sigma x^\gamma\partial_\sigma x^\delta)]^{1/2} \equiv -\mu\int d\sigma\, d\tau(-h)^{1/2}\ . \tag{3.1}$$

Here $-h$ is the determinant of the induced metric on the world sheet, given by $h_{ij}=g_{\mu\nu}\partial_i x^\mu\partial_j x^\nu$. From dimensional considerations, μ has dimensions mass/length, and can be identified with the mass per unit length of the cosmic string. The energy-momentum tensor that follows from (3.1) is given by[12]

$$T^{\mu\nu}=\mu\int d\sigma\, d\tau(-h)^{1/2}\delta^4(x^\mu-x^\mu(\sigma,\tau)) \times[(g_{\alpha\beta}\partial_\sigma x^\alpha\partial_\sigma x^\beta)\partial_\tau x^\mu\partial_\tau x^\nu +(g_{\alpha\beta}\partial_\tau x^\alpha\partial_\tau x^\beta)\partial_\sigma x^\mu\partial_\sigma x^\nu -(g_{\alpha\beta}\partial_\tau x^\alpha\partial_\sigma x^\beta)(\partial_\tau x^\mu\partial_\sigma x^\nu+\partial_\sigma x^\mu\partial_\tau x^\nu)]\ . \tag{3.2}$$

Using the Euler-Lagrange equations to minimize the action yields the equations of motion

$$\partial_\tau\{(-h)^{-1/2}[(g_{\alpha\beta}\partial_\tau x^\alpha\partial_\sigma x^\beta)g_{\mu\nu}\partial_\sigma x^\nu-(g_{\alpha\beta}\partial_\sigma x^\alpha\partial_\sigma x^\beta)g_{\mu\nu}\partial_\tau x^\nu]\} +\partial_\sigma[(-h)^{-1/2}((g_{\alpha\beta}\partial_\tau x^\alpha\partial_\sigma x^\beta)g_{\mu\nu}\partial_\tau x^\nu-(g_{\alpha\beta}\partial_\tau x^\alpha\partial_\tau x^\beta)g_{\mu\nu}\partial_\sigma x^\nu)] =(-h)^{-1/2}\partial_\mu g_{\alpha\beta}[(g_{\gamma\delta}\partial_\tau x^\gamma\partial_\sigma x^\delta)\partial_\tau x^\alpha\partial_\sigma x^\beta-\tfrac{1}{2}(g_{\gamma\delta}\partial_\sigma x^\gamma\partial_\sigma x^\delta)\partial_\tau x^\alpha\partial_\tau x^\beta-\tfrac{1}{2}(g_{\gamma\delta}\partial_\tau x^\gamma\partial_\tau x^\delta)\partial_\sigma x^\alpha\partial_\sigma x^\beta]\ . \tag{3.3}$$

This equation can be simplified by the traditional choice of gauge,

$$g_{\alpha\beta}\partial_\tau x^\alpha\partial_\sigma x^\beta=0\ , \tag{3.4}$$

$$g_{\alpha\beta}(\partial_\tau x^\alpha\partial_\tau x^\beta+\partial_\sigma x^\alpha\partial_\sigma x^\beta)=0 \tag{3.5}$$

to

$$(\partial_\tau^2-\partial_\sigma^2)x^\mu=-\Gamma^\mu_{\alpha\beta}(\partial_\tau x^\alpha\partial_\tau x^\beta-\partial_\sigma x^\alpha\partial_\sigma x^\beta)\ . \tag{3.6}$$

Here $\Gamma^\mu_{\alpha\beta}\equiv\frac{1}{2}g^{\mu\gamma}(\partial_\alpha g_{\gamma\beta}+\partial_\beta g_{\gamma\alpha}-\partial_\gamma g_{\alpha\beta})$ is the Christoffel affine connection. We make a transformation to new coordinates u and v by defining $u\equiv\tau+\sigma, v\equiv\tau-\sigma$. These are "light-cone" coordinates, since they are null by virtue of conditions (3.4) and (3.5), which become

$$g_{\alpha\beta}\partial_u x^\alpha\partial_u x^\beta=0\ , \tag{3.7}$$

$$g_{\alpha\beta}\partial_v x^\alpha\partial_v x^\beta=0\ . \tag{3.8}$$

With these conditions, (3.6) becomes

$$\partial_u\partial_v x^\mu=-\Gamma^\mu_{\alpha\beta}\partial_u x^\alpha\partial_v x^\beta\ . \tag{3.9}$$

This equation of motion preserves the gauge choice $\partial_u(g_{\mu\nu}\partial_v x^\mu\partial_v x^\nu)=0$ and $\partial_v(g_{\mu\nu}\partial_u x^\mu\partial_u x^\nu)=0$. Equation (3.9) can be more elegantly written as the covariant generalization of the flat-space equation of motion for the cosmic string:

$$D_u(\partial_v x^\mu)=0\ . \tag{3.10}$$

The null four-vectors $\partial_u x^\mu$ and $\partial_v x^\mu$, are parallel transported along geodesics in the background metric. Since parallel transport preserves the norm of any four-vector, the gauge conditions are preserved over time.

In the back-reaction problem, the string is itself the source of the gravitational field determining its motion. Its stress energy determines $\Gamma^{\mu}_{\alpha\beta}$. Since the gravitational back-reaction effects can be expanded in terms of the main dimensionless parameter in the problem, namely, $G\mu\sim 10^{-6}$, we use linear gravity to compute the metric and to evolve the string iteratively.

Expanding the metric in the usual fashion as $g_{\mu\nu}=\eta_{\mu\nu}+h_{\mu\nu}$. The linearized equations of general relativity are[13]

$$\Box h_{\mu\nu}=-16\pi G(T_{\mu\nu}-\tfrac{1}{2}\eta_{\mu\nu}T^{\alpha}_{\alpha})\equiv -16\pi S_{\mu\nu} \ . \tag{3.11}$$

In the light-cone gauge, the energy-momentum tensor from (3.2) is given by[12]

$$T^{\mu\nu}(x^{\alpha})=\mu\int du\, dv(\partial_u z^{\mu}\partial_v z^{\nu}+\partial_v z^{\mu}\partial_u z^{\nu}) \times\delta^4(x^{\alpha}-z^{\alpha}(u,v)) \ . \tag{3.12}$$

Throughout this paper, x denotes field points, and z denotes source points. The retarded Green's function technique[14] yields

$$h_{\mu\nu}(x^{\alpha})=8G\mu\int du\, dv\, F_{\mu\nu}(z(u,v)) \times\theta(x^0-z^0)\delta((x-z)^2) \ , \tag{3.13}$$

where

$$F_{\mu\nu}\equiv\partial_u z_{\mu}\partial_v z_{\nu}+\partial_v z_{\mu}\partial_u z_{\nu}-\eta_{\mu\nu}\partial_u z^{\alpha}\partial_v z_{\alpha} \ .$$

Turok uses this approach in his calculation of the gravitational field near an unperturbed oscillating string.[15] Note that (3.11) requires the harmonic gauge condition $\partial^{\alpha}h_{\mu\alpha}=\frac{1}{2}\partial_{\mu}h^{\alpha}_{\alpha}$ which is satisfied by (3.13) as long as $T^{\mu\nu}$ is confined to a finite volume in space.[13]

Equation (3.13) is an integral which sums contributions from source points along the intersection of the string world sheet and the past light cone of x^{α}, the field point. This simply expresses the fact that gravitational interactions in the linear regime propagate at the speed of light and that we believe in causality. Since we are in the linear regime, $h_{\mu\nu}$ and $\Gamma^{\mu}_{\alpha\beta}$ are proportional to $G\mu\sim 10^{-6}$ and are small. To first order in $G\mu$ we can then write (3.9) as

$$\partial_u\partial_v x^{\mu}=-\tfrac{1}{2}\eta^{\mu\gamma}(\partial_{\alpha}h_{\beta\gamma}+\partial_{\beta}h_{\alpha\gamma}-\partial_{\gamma}h_{\alpha\beta})\partial_u x^{\alpha}\partial_v x^{\beta} \ , \tag{3.14}$$

where, from (3.13), we have

$$\partial_{\gamma}h_{\mu\nu}=8G\mu\int du\, dv\, F_{\mu\nu}(z(u,v)) \times\partial_{\gamma}[\theta(x^0-z^0)\delta((x-z)^2)] \ . \tag{3.15}$$

Equations (3.14) and (3.15) are the master equations that must be solved in treating the gravitational back-reaction problem. The first gives the motion of the string in its own field, and the second gives the field in terms of the motion of the string. The rest of the paper is devoted to iteratively solving these equations for different initial string trajectories.

IV. DYNAMICS OF SELF-INTERACTING STRINGS

We begin with an unperturbed string solution $x^{\mu}_0(u,v)$ that obeys the wave equation $\partial_u\partial_v x^{\mu}_0=0$ and satisfies the conditions (3.7) and (3.8) in flat space:

$$\eta_{\mu\nu}\partial_u x^{\mu}_0\partial_u x^{\nu}_0=0, \quad \eta_{\mu\nu}\partial_v x^{\mu}_0\partial_v x^{\nu}_0=0 \ . \tag{4.1}$$

x^{μ}_0 is only the zeroth-order approximation to the true solution, exact in the limits $G\mu\to 0$. We use x^{μ}_0 as the source to compute the string gravitational field to order $G\mu$. We then use this gravitational field to calculate the leading-order term in string evolution.

Averaging over a period, we find the leading-order change in the trajectory:

$$\Delta(\partial_u x^{\mu}_0)=\int_0^1 dv\, \partial_u\partial_v x^{\mu} =-\tfrac{1}{2}\int_0^1 dv(\partial_{\alpha}h^{\mu}_{\beta}-\partial^{\mu}h_{\alpha\beta})\partial_u x^{\alpha}\partial_u x^{\beta} \ . \tag{4.2}$$

Since $h_{\alpha\beta}$ is a functional of a periodic trajectory, the second term in (3.14) vanishes as a total derivative. The new solution $\partial_u x^{\mu}_0+\Delta(\partial_u x^{\mu}_0)$ again satisfies the gauge conditions to order $G\mu$: $\eta_{\mu\nu}\Delta(\partial_u x^{\mu})\partial_u x^{\nu}$ vanishes by antisymmetry. $\Delta\partial_v x^{\mu}_0$ also modifies the initial solution in a gauge-perserving manner. We can then repeat the procedure, using the new solution as a source for the gravitational field, and compute its effect over a period, obtaining again another solution. Each time the new solution differs from the old by a term proportional to $G\mu$, which is nominally small, and so we trace the evolution of the trajectory from period to period in a gradual way.

This iterative approach is only valid when the back reaction is finite. In Appendix A, we argue that there is no short-distance divergence in $\partial_u\partial_v x^{\mu}$. The points along the u branch of the light cone contribute a finite "tidal" acceleration:

$$\partial_u\partial_v x^{\mu}\sim\tfrac{7}{6}G\mu\frac{\partial_u x^{\alpha}\partial_u^3 x_{\alpha}}{(\partial_u x^{\alpha}\partial_v x_{\alpha})^2} \times(\partial_u x^{\alpha}\partial_v^2 x_{\alpha}\partial_v x^{\mu}-\partial_u x^{\alpha}\partial_v x_{\alpha}\partial_v^2 x^{\mu})\int_u^0 du\, u \ . \tag{4.3}$$

A corresponding term is contributed by points along the v branch. Equation (4.3) shows that the contribution to the back-reaction force from nearby points is finite, and *indeed goes to zero* as the source point approaches the field point.

This argument fails at the cusp, where a point on the string moves at the speed of light and we can no longer boost into the frame that is locally Minkowskian: $\partial_u x^{\alpha}\partial_v x_{\alpha}$ vanishes and $\partial_u\partial_v x^{\mu}$ diverges. However, since the radiation from the cusp is finite,[16] the energy loss and the work done from the back reaction is finite, and the singularity in $\partial_u\partial_v x^{\mu}$ is an integrable one. This may be checked by expanding (4.3) at points around the cusp, and numerically by studying the change in position of points on the world sheet immediately around the cusp. We find no surprises as we probe around the cusp.

Gravitational back reaction both shrinks the string and accelerates it, because the string radiates both energy and momentum. The change in the string four-momentum,

$$P^{\mu}\equiv\int d^3x\, T^{\mu 0}\ , \tag{4.4}$$

can be computed from the force density

$$\partial_\nu T^{\mu\nu}=2\mu\int du\, dv\, \partial_u\partial_v x^{\mu}\delta^4(x^{\alpha}-z^{\alpha}(u,v))\ , \tag{4.5}$$

where $T^{\mu\nu}$ is the string stress energy density. Combining (4.5) with (4.4) and invoking Gauss's divergence theorem, we obtain the important relation

$$\Delta P^{\mu}=2\mu\int du\, dv\, \partial_u\partial_v x^{\mu}\ . \tag{4.6}$$

Here the change in four-momentum of the string is defined over one period, so that the integration region in (4.6) is over the range in u and v corresponding to σ going from 0 to 1, and τ going from 0 to $\frac{1}{2}$, i.e., u and v ranging from 0 to 1.

In Appendix B, we show that (4.6) is equivalent to the standard expression[13] for power radiated by a moving body. However, this formulation has the advantage that both the motion of the string and its energetics can be traced over time. In particular, the velocity of the center of mass of the string is simply given by $v^i\equiv P^i/P^0$. With (4.6), it is possible to track the motion of the center of mass of the string, and study the *rocket effect*. If the rocket effect is large, it can have important consequences for the cosmic-string scenario of galaxy formation, particularly with hot dark matter.[17]

One final note on the dynamics of self-interacting strings concerns the role of time. While it is possible to identify the timelike world-sheet coordinate τ with the actual laboratory time t in the case of the noninteracting string, this definition does not hold for the interacting string. This follows from Eq. (3.14). Time, as the other three space coordinates, is also affected by the back reaction. In particular, every new solution obtained from the previous old solution has radiated some energy, and hence has shrunk. Thus its period in *real time* t has diminished, and yet as outlined above, each of these solutions is always periodic in *coordinate time* τ with period $\frac{1}{2}$. Hence the net effect of the back reaction on time is to shrink the proportion between t and τ. Also, after each interaction, the relation between t and τ is skewed, in the sense that the loop τ=const is not the same as t=const. However, it is always possible to redefine time so that $t=\text{const}\times\tau$. This eases the presentation of the loop trajectories, which are parametrized by σ and τ, so that looking at a trajectory at τ=const is the same as looking at the loop at a given time. Below, we shall present the shapes of string loops, showing how they look at given slices of real time. After each iteration, we have corrected for the skewing between t and τ.

We now turn to discussing the numerical implementation of these concepts and present our results.

V. NUMERICAL IMPLEMENTATION—THE CODE

In order to evolve the string trajectory numerically, we must evaluate the back-reaction force $\partial_u\partial_v x^{\mu}$ and compute the change in the trajectory after each period. Hence the code consists of two parts. The first is devoted to the evaluation of $\partial_u\partial_v x^{\mu}$, and the second is devoted to the integration of (4.2). There are two versions of the code: in one representation, the string's world sheet is a continuous, differentiable function. In the other representation, the string is discretized into segments that are piecewise constant.[18,19]

A. Evaluating $\partial_u\partial_v x^{\mu}$

Each point along the string experiences an acceleration due to the "tidal" force exerted by all points along its past light cone. For every field point, we need to trace the null curve and evaluate the contribution of each source point.

In the continuous case, the null curve is divided into three parts. We begin by integrating along the null curve with du as our integration variable, using the Newton-Raphson method,[20] to find $v(u)$ such that $f\equiv[x-z(u,v(u))]^2=0$. We then change the integration variable to $d\sigma$, use the nullity condition to find $\tau(\sigma)$, and integrate further along the curve. Finally, we use dv as the integration coordinate, compute $u(v)$, and integrate back to the field point. The only subtlety here is that the change of variables between branches entails a change of integration region, and hence the boundary terms in (A3) must be included. There are two boundary terms, arising at the connection between the σ branch and the u and v branches.

We needed to divide the integration into three pieces to avoid numerical singularities. The integral in (A4), rewritten in σ-τ coordinates, diverges logarithmically at short distances. While there is a boundary term from (A3) which formally cancels this divergence, evaluating this cancellation numerically is disastrous, entailing a difference between two large numbers. In u-v coordinates, the boundary terms disappear to begin with, and the integrand in (A4) is well behaved. The advantage of working with the light-cone coordinates is clear; hence the necessity to divide the integration region into three parts:

In the discrete case, the situation simplifies tremendously. The world sheet is a polyhedron, made up of plane surfaces. It is no longer necessary to trace the entire null curve in order to compute $\partial_u\partial_v x^{\mu}$, using very small steps to accurately evaluate an oscillating integral. Instead, we can rewrite (A4) as a discrete sum of contributions from each of the flat pieces of the world sheet. Thus, we can quickly compute $\partial_u\partial_v x^{\mu}$ for the kinky world sheet by summing over left- and right-moving kinks that lie on the null curve of the field point. The only subtlety here is keeping track of whether the kinks on the null curve are left or right moving—each demands its appropriate boundary term [see Eq. (A3)].

We now give a short description of the behavior of Eq. (A4) in the case of kinky strings. In this case, the derivatives $\partial_u z^{\mu}$ and $\partial_v z^{\mu}$ are piecewise constant, and hence so is $F_{\mu\nu}(u,v)$. Hence one can sum the contributions to $\partial_\gamma h_{\alpha\beta}$ from regions where $F_{\mu\nu}$ is constant. In this case, Eq. (A4) reduces to a sum of terms proportional to

$$\partial_\gamma h_{\alpha\beta} \propto F_{\alpha\beta} \partial_v z_\gamma \int \frac{du}{(\partial_v f)^2} \tag{5.1}$$

which can be integrated immediately since f is a simple function of u and v when the world sheet is a plane surface. After boundary terms are included (when a u kink follows a v kink, for instance), $\partial_u \partial_v x^\mu$ can be obtained as a sum over kinks lying on the null curve. In such a manner, the back reaction can be computed very quickly for kinky trajectories.

In the discrete case, there is no need to worry about canceling divergences near the field point: since we can always boost to a frame where a segment of the string is at rest, the self-force of a straight segment vanishes.

B. Integrating $\partial_u \partial_v x^\mu$

This is the main routine of our code. $\partial_u \partial_v x^\mu$ is computed over a periodic grid in u and v. For each value of u or v, the back reaction $\partial_u \partial_v x^\mu$ is integrated over a unit interval in v or u. Since $\partial_u \partial_v x^\mu$ is periodic, the new trajectory is guaranteed to be periodic and closed. This new trajectory then is ready to be used in (3.15) to find yet another trajectory, one period later. In this manner, we evolve the shape of the string in steps of time that are one period long.

In the discrete code, $\partial_u x^\mu$ and $\partial_v x^\mu$ are represented as piecewise constant functions. A trajectory is defined by specifying $\partial_u x^\mu$ at N equally spaced points, u_i, along the u unit interval and $\partial_v x^\mu$ at N points, v_j, along the v unit interval. Summing along the string world lines, we determine the change in the trajectory at each point:

$$\Delta[\partial_u x^\mu(u_i)] = \frac{1}{N} \sum_{j=1}^{N} \partial_u \partial_v x^\mu(u_i, v_j) ,$$

$$\Delta[\partial_v x^\mu(v_j)] = \frac{1}{N} \sum_{i=1}^{N} \partial_u \partial_v x^\mu(u_i, v_j) .$$

This formulation assures string closure:

$$\Delta \oint \partial_\sigma x^\mu d\sigma = \tfrac{1}{2} \oint (\Delta \partial_u x^\mu - \Delta \partial_v x^\mu) d\sigma$$
$$= \frac{1}{2N} \sum_{i=1}^{N} \sum_{j=1}^{N} \partial_u \partial_v x^\mu(u_i, v_j) - \frac{1}{2N} \sum_{j=1}^{N} \sum_{i=1}^{N} \partial_u \partial_v x^\mu(u_i, v_j) = 0 .$$

If we had removed the second term of $\partial_u \partial_v x^\mu$ in (3.14) for the u derivatives and the first term of $\partial_u \partial_v x^\mu$ for the v derivatives, the code would have strictly preserved the gauge conditions. However, the $\Delta[\partial_u x^\mu(u_i)]$ and $\Delta[\partial_v x^\mu(v_j)]$ would lose their symmetry and the string would no longer exactly close. (Closure would occur only in the limit of $N \to \infty$.) We chose instead not to tamper with $\partial_u \partial_v x^\mu$, and not to remove any terms which in the $N \to \infty$ limit should go to zero. This keeps the string closed, but after every period a slight correction was made to ensure that the gauge conditions (4.1) were identically satisfied. In the next section, we use the gauge condition as a check on the code.

Finally, by integrating over the whole period [see Eq. (4.6)], the energy and momentum lost by the string can be computed:

$$\Delta P^\mu = \frac{2}{N^2} \sum_{i=1}^{N} \sum_{j=1}^{N} \partial_u \partial_v x^\mu(u_i, v_j) .$$

Thus the energetics of the string, i.e., its radiative power, also can be traced over time. Also, the change in center-of-mass velocity of the string loop can be calculated.

On a CONVEX C110, with vector optimization, the discrete code takes 15 sec to complete a time step for an $N=16$ grid. The CPU time scales as N^3. On a SUN4/110, a time step in the discrete code takes about one minute with the same grid.

C. Consistency checks

Symmetries of the back-reaction problem, existing numerical work, and some of the analytical work outlined in the paper provide rigorous tests of the computer code and the numerical method.

First, the behavior of the integrand in Eq. (3.14) was studied near the filed point. All divergences disappear and the behavior of $\partial_u \partial_v x^\mu$ is correctly described by the analytic limit given by (4.3).

Next, after every new trajectory was obtained, we computed the errors in the gauge conditions. In the limit of large N, both products $\eta_{\mu\nu} \Delta(\partial_u x^\mu) \partial_u x^\nu$ and $\eta_{\mu\nu} \Delta(\partial_v x^\mu) \partial_v x^\nu$ should approach zero, since each term is the integral of a total derivative. Since our integration is simply a sum over N points in the unit interval in Eq. (4.2), we are replacing an integral which should be zero by a sum of terms which should approximately add to zero. As N was increased, the products above did go to zero. With $N=16$, these were typically of order 0.05. With $N=32$ points, they were small, typically of order 0.01 or less, and with $N=64$, they were less than 0.002.

A third check was to verify Lorentz invariance of the code. All of the key relations, e.g., (3.14), (3.15), (4.6), and (A1), are strictly written in a covariant way. Thus all four-vectors, such as energy momentum radiated in one period, should Lorentz boost properly, and scalars such as gravitational power, should remain constant. Using the same string trajectory, but Lorentz boosted into a different frame, we checked that this was indeed true. All physical quantities transformed correctly. Our code is exactly Lorentz covariant.

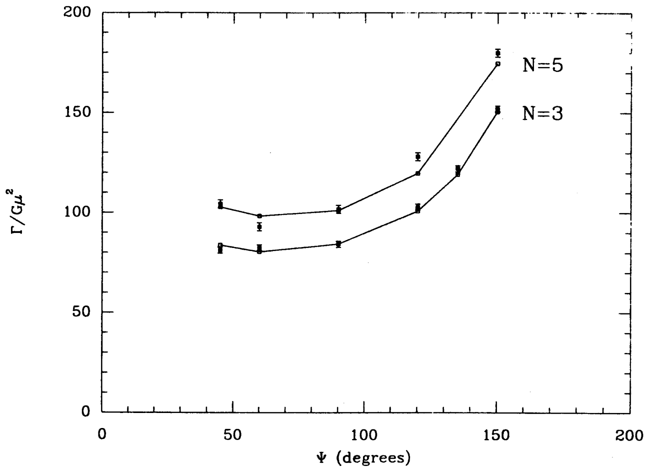

FIG. 1. Γ vs ψ for the $N=3$ (lower) and $N=5$ families of Burden trajectories. Γ is in units of $G\mu^2$. Open squares are Burden's results (no errors quoted). Solid squares are our results.

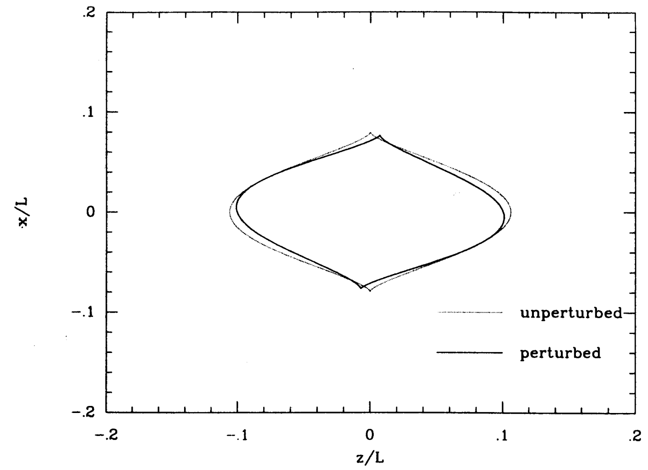

FIG. 2. x-z projection of the $N=3$, $\psi=\pi/2$ Burden trajectory, unperturbed (symmetric) and perturbed. $G\mu$ is taken to be 10^{-3}. Both axes are in units of L.

As a final check of our formalism, we compared the power radiated by a Burden string loop trajectory to previously calculated values.[21] The Burden trajectories are given by

$$\begin{aligned}\mathbf{a}(u)&=\frac{N^{-1}}{2\pi}[\cos(2\pi Nu)\hat{\mathbf{z}}\\&\qquad+\sin(2\pi Nu)(\cos\psi\hat{\mathbf{x}}+\sin\psi\hat{\mathbf{y}})]\ ,\\\mathbf{b}(v)&=\frac{M^{-1}}{2\pi}[\cos(2\pi Mv)\hat{\mathbf{z}}-\sin(2\pi Mv)\hat{\mathbf{x}}]\ .\end{aligned}\tag{5.2}$$

These are nonintersecting cuspy loops in the case $M=1$ and $N>1$, and ψ not equal to 0 or π.

Burden used the standard expression[13] for the gravitational power and summed over modes and integrated over solid angle.[21] The convergence in mode number is very slow (going as $n^{-1/3}$ where n is the mode number), due to the presence of cusps on the string, and no errors are quoted in the paper. The open squares in Fig. 1 are from Burden's calculation[21] of $\Gamma\equiv P/G\mu^2$ for the $N=3$ and $N=5$ trajectories as a function of ψ (here $M=1$). The filled squares are our results for the same trajectories, where we have substituted (5.2) as a zeroth-order solution into (3.14) and (3.15), and integrated (4.6) over one period. We find excellent agreement between the two sets of results.

VI. RESULTS—DECAY OF SMOOTH LOOPS

In this section, we explore the evolution of kinkless strings. We will use both the discrete and continuous string representations to study the evolution of cusps, the long-term evolution of strings and the rocket effect. The continuous representation is a more accurate portrayal of the cusp; however, evolving this representation is extremely time consuming—we need to evaluate an integral with an oscillating integrand and, at each point in the evaluation of the integrand, we need to evaluate $\partial_u x^\mu$ and $\partial_v x^\mu$, which are sums of N Fourier terms.

A. The back reaction and cusps

Using the continuous representation of the string, we explored the effects of gravitational back reaction on the cusps, focusing on the evolution of the Burden trajectories. These trajectories, defined in (5.2), are a sum of simple trigonometric functions. Using the method outlined in Sec. V, we calculated (3.15) using Romberg integration[22] to extrapolate the value of $\partial_u\partial_v x^\mu$ at N^2 points on the u,v grid.

While $\partial_u\partial_v x^\mu$ is finite away from the cusps, it diverges directly on the cusp, so we select the grid of N^2 points so that it straddles cusp points. However, as the singularity evolved is integrable, the high-N limit should adequately represent the exact effect of back reaction on cusps. Then, taking the Fourier transform of (3.14), it can be shown[23] that the coefficients of the Fourier modes of the perturbed trajectory are directly related to the Fourier transform coefficients of $\partial_u\partial_v x^\mu$. In this manner, we performed a mode analysis of the back reaction on cusps,

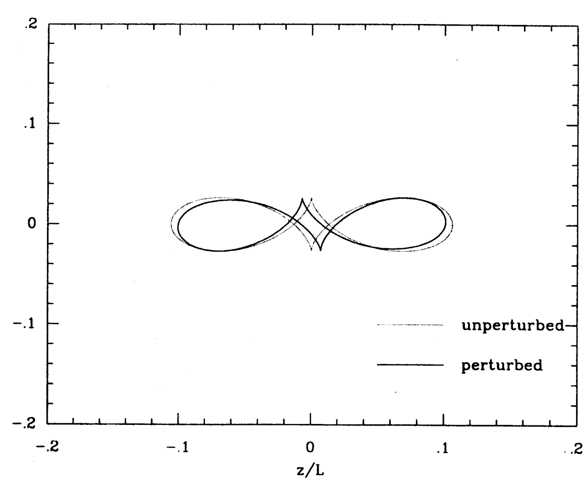

FIG. 3. y-z projection with the same parameters as Fig. 2.

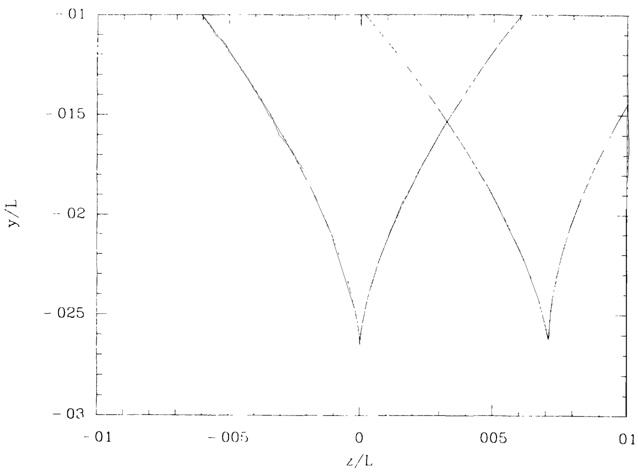

FIG. 4. Blow up of Fig. 3, showing the survival, but delay and deformation of, the cusp.

and found that the perturbed mode coefficients scale like $a_n \sim n^{-4/3}$, and converge reasonably rapidly. This means that after 100 moves ($N=100$ above), the perturbed trajectory is known to better than 1%.

Using this approach, we trace the evolution of a cusp over a single cycle. Figures 2 and 3 show the effect of the back reaction on the cusps of the $(M=1, N=3, \psi=\pi/2)$ Burden trajectory. This is the effect the back reaction would have after one period (time $L/2$) if $G\mu$ were 10^{-3}. In most string models, $G\mu \sim 10^{-6}$, and so these figures show the effect of back reaction after about 1000 periods of a realistic cosmic-string loop. Figure 4 is a blowup of Fig. 3. Clearly, the cusp survives the back reaction, but is deformed and delayed. Our numerical results are in agreement with the analytical arguments of Thompson,[24] claiming that cusps would survive the back reaction. Indeed, they do.

After one cycle, the input string solution, $\partial_u x_0^\mu$, is a function not of three Fourier terms, but rather N Fourier terms. This slows the code by a factor $N/3$ and makes further evolution of the string with the continuum version of the code numerically prohibitive, even on a minisupercomputer.

B. Decay of simple loops

We have also explored the long-term evolution of string trajectories. Using the discrete representation, we evolve the string until it decays to a small fraction of its initial mass or until it self-intersects.

Figures 5 and 6 show the evolution of the discretized $N=3$ and $N=5$ Burden trajectories, which are represented with 16 segments. Since these are relatively

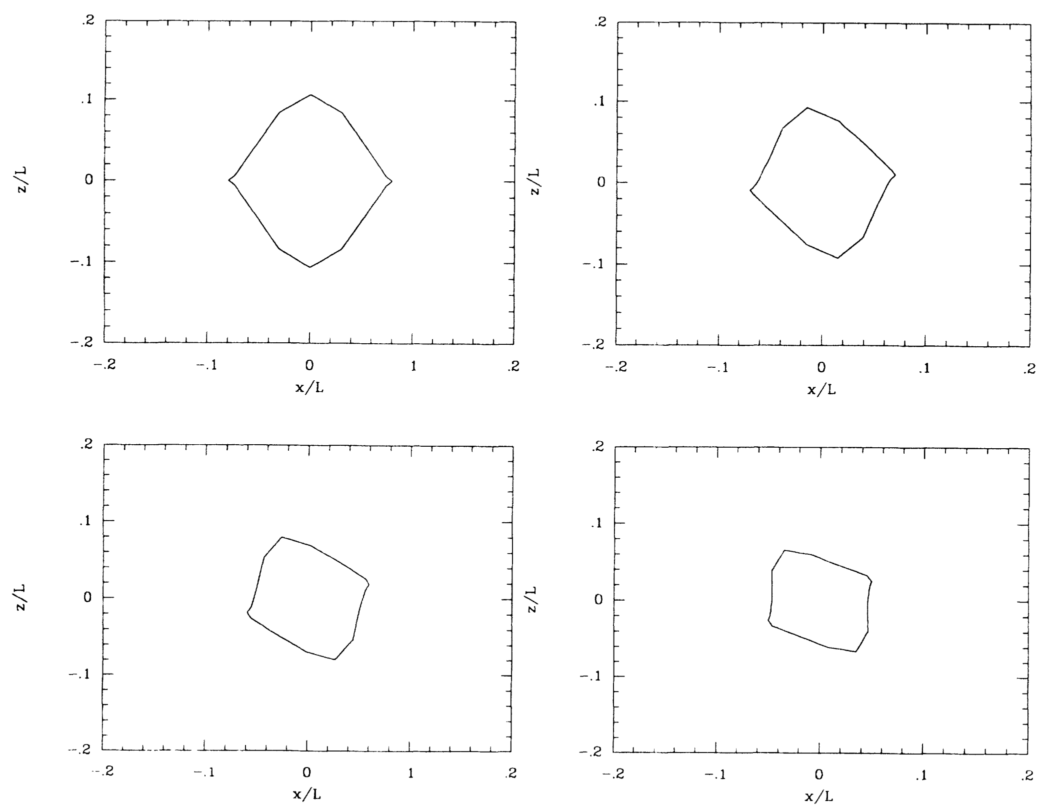

FIG. 5. x-z projection of the evolution of the $N=3$, $\psi=\pi/2$ Burden trajectory, where each step is $10^{-3}/G\mu$ periods. Here 16 segments have been used.

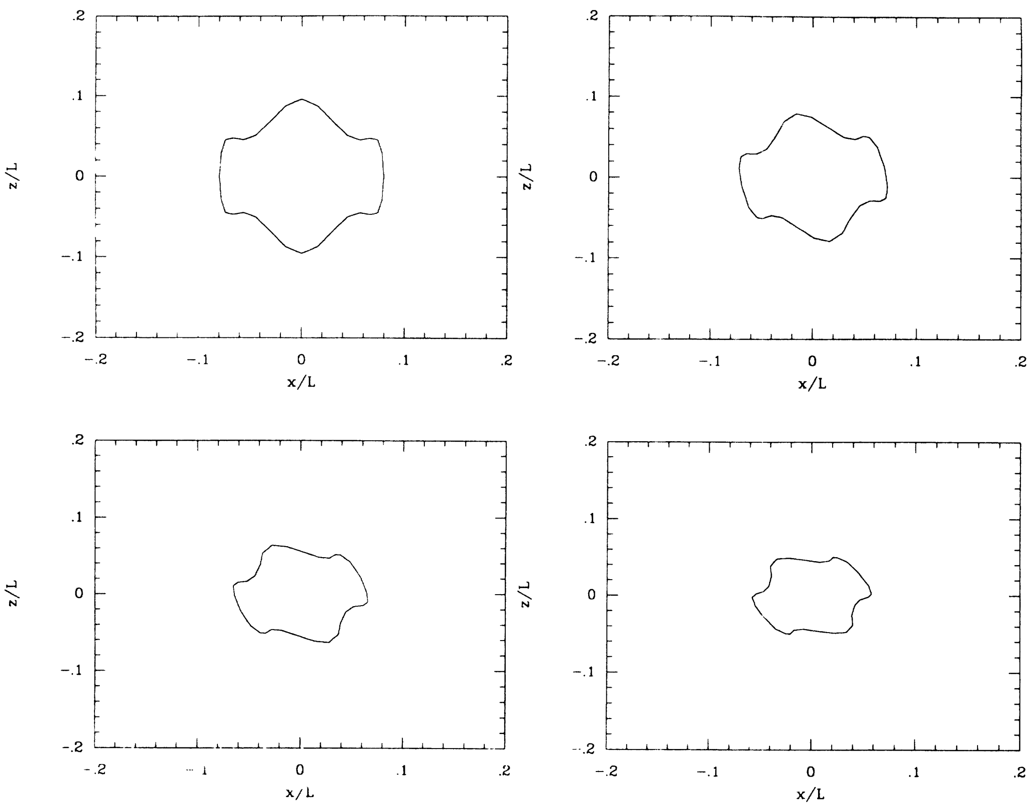

FIG. 6. x-z projection of the $N=5, \psi=\pi/2$ Burden trajectory, with the same time step as Fig. 5. Here 16 segments have been used.

smooth and simple trajectories, the evolution is insensitive to the segment size. While discretization removes the cusps in the original Burden trajectory, there are still many points along the string that are moving at ultrarelativistic velocities somewhere along the trajectory. We evolved these string loops using steps of $10^{-3}/G\mu$ string periods. At first, the trajectory in Fig. 5 distorts, as the back reaction twists the string somewhat, but soon it relaxes into an almost self-similar solution, slowly decaying at a constant rate.

Because of the gauge conditions, it is difficult to decompose a string into low- and high-frequency components. "Crinkliness" is a more useful measure of the string's small-scale structure.

Figure 7 shows the loss of energy of the loop in Fig. 5 as it decays, and Fig. 8 the shift in Γ, the power

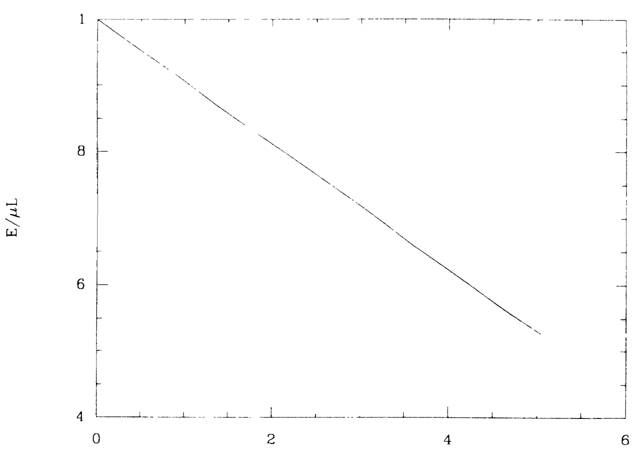

FIG. 7. Energy of the loop in Fig. 6 as a function of time. Energy is in units of μL, the initial energy of the string, and time in units of $L\times(10^{-3}/G\mu)$.

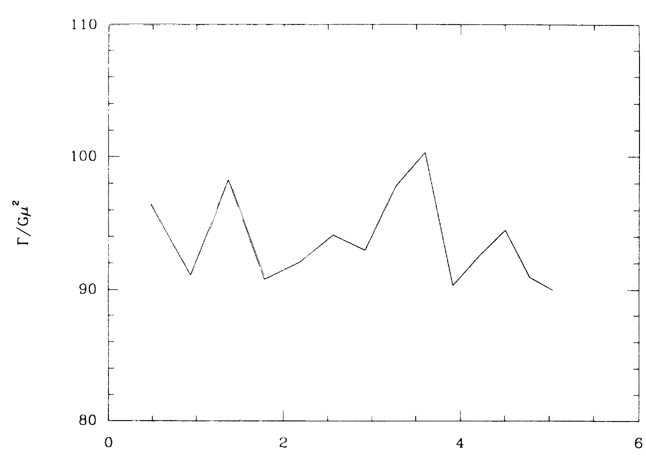

FIG. 8. Power of the loop in Fig. 5 as a function of time. Power is in units of $G\mu^2$.

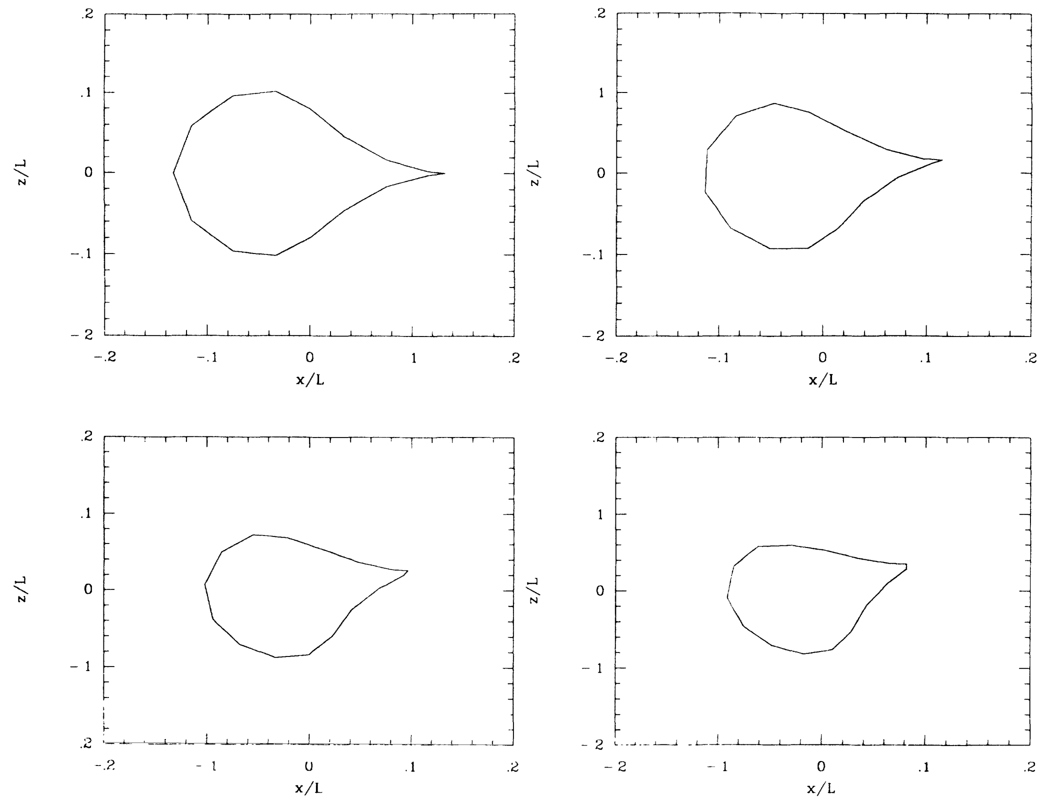

FIG. 9. x-z projection of an asymmetric trajectory, $\alpha=0.5$ and $\phi=\pi/2$, with the same units as Fig. 2.

coefficient described earlier. This coefficient does tend to relax somewhat towards what appears to be a typical value of around 70.

C. Rocket effect

Asymmetric string trajectories radiate not only energy, but also momentum. This radiation might accelerate string loops to relativistic velocities, thus modifying their role as seeds for galaxy formation.[25]

In order to explore the rocket effect, we studied the evolution of an asymmetric two-parameter family of solutions described by Vachaspati and Vilenkin:[16]

$$\mathbf{a}(u)=\frac{1}{2\pi}[\sin(2\pi u)\hat{\mathbf{x}}-\cos(2\pi u)(\cos\phi\hat{\mathbf{y}}+\sin\phi\hat{\mathbf{z}})] , \tag{6.1}$$

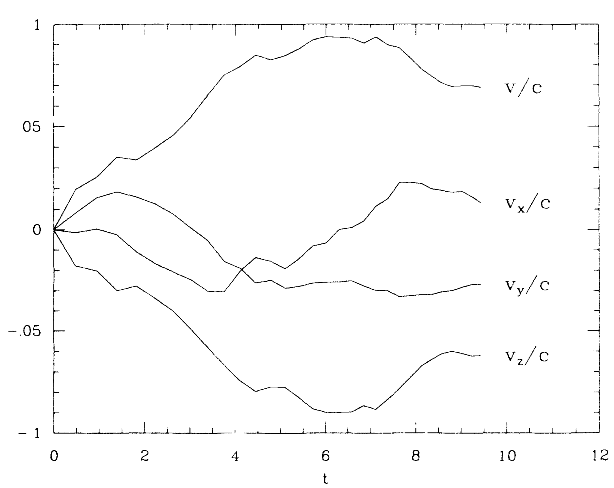

FIG. 10. x,y,z velocities of the center of mass of the loop in Fig. 9, in units of c; the upper curve is the speed.

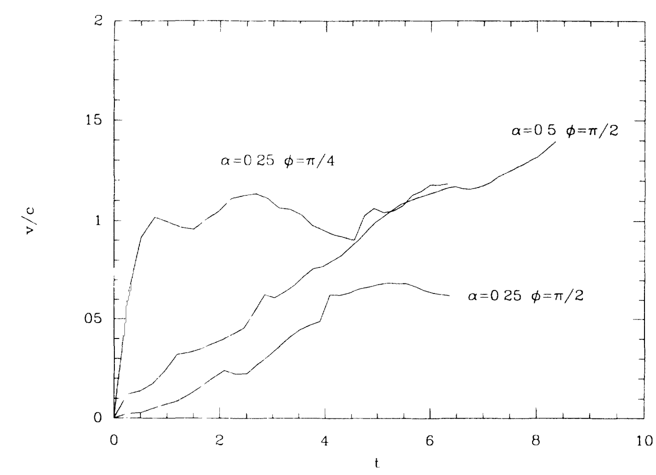

FIG. 11. Center-of-mass velocities for several asymmetric trajectories.

$$\mathbf{b}(v) = \frac{1}{2\pi}[(1-\alpha)\sin(2\pi v) - (\alpha/3)\sin(6\pi v)]\hat{\mathbf{x}} + \frac{1}{2\pi}\{[(1-\alpha)\cos(2\pi v) + (\alpha/3)\cos(6\pi v)]\hat{\mathbf{y}} + [\alpha(1-\alpha)]^{1/2}\sin(4\pi v)\hat{\mathbf{z}}\} .$$

These trajectories, if they did not evolve, would eventually reach relativistic velocities as they decay.

We evolved these loops over a decay time and found that the asymmetric terms are gradually suppressed by gravitational back reaction. The amplitude of the cusp are suppressed and the location of the cusp processes—these two effects limit the rocket effect. Figure 9 shows the evolution of the $(\alpha=0.5, \phi=\pi/2)$ trajectory. The center of mass is always shown at the origin. Figure 10 shows the various components of the center-of-mass velocity of this trajectory. After the loop has lost more than half its energy, the velocity is of order $0.1c$, a result consistent with heuristic estimate.[26] Figure 11 follows the evolution of several different trajectories—the center-of-mass velocity grows towards $\sim 0.1c$ and then saturates near this value.

VII. RESULTS—KINKY LOOPS

A. Evolution of kinky loops

Numerical simulations of string evolution[4] suggest that kinks play a dominate role in the evolution of strings. As the simulations progress, the long strings become increasingly crinkly and the loops produced by fragmentation are an ever smaller fraction of the horizon. The simulations suggest that loops produced today would be a miniscule fraction of the horizon. The cosmological simulations, however, do not include back-reaction effects. These effects will alter the behavior of the kinks and will determine the final outcome of the scaling solution. (Of course, since gravitational back-reaction effects have not been included in numerical simulations, the existence of a scaling solution has not been rigorously established. For example, the number of long strings per unit horizon volume may grow logarithmically. This logarithmic growth correction occurs in domain-wall evolution.[27])

The importance of kinks motivates our study of their evolution. In the previous section, we discussed the evolution of rather smooth trajectories, which we took to be the Burden trajectories of (5.2), approximating these by a collection of small straight segments. There, discontinuities in the tangent direction were small. The decay of these loops is uneventful; rapidly, the power radiated converges to a fixed value, and the loops decay almost in a self-similar manner. Here, we are interested in the decay of loops which have real, sharp kinks.

We begin with the Burden trajectories, taking $\mathbf{b}(v)$ as given in (5.2) by $M=1$, which is simply a rotating circle. We then superimpose on this a sawtooth wave form $\mathbf{s}$, adding it to both $\mathbf{a}(u)$ and $\mathbf{b}(v)$. This sawtooth function has N teeth on it, in the interval 0 to 1. The "tooth an-

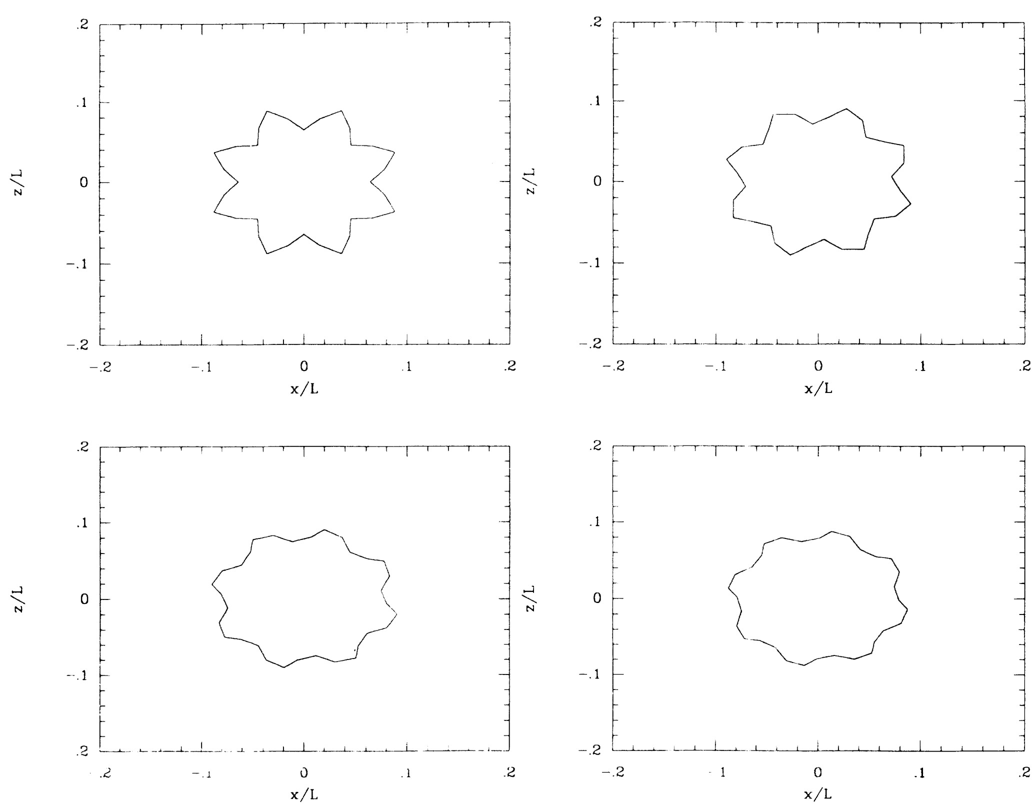

FIG. 12. Composite, showing the decay of a kinky string loop with 8 kinks on it. Each graph is separated in time by $10^{-3}/G\mu$ periods. Axes are in units of L.

gle" can be varied; we have varied it from 30 to 120 deg. After adding such a function, the gauge conditions (4.1) are perturbed and no longer satisfied. Hence, after perturbing the Burden trajectory with a kinky sawtooth, we correct for the gauge conditions by altering the magnitude and direction of the initial velocities of the segments.

We compute the back reaction and evolve the loop. The small kinks decay more rapidly than the string. Figure 12 shows the evolution of a kinky loop with 8 kinks on it. (Here the x-z projection only is shown. There is kinky structure in the y-z plane as well, and as the loop decays, that structure also disappears, and the string is approximately circular in the x-z plane.) We used 32 segments in all to represent the string, thus using 4 segments per kink to sample the discontinuities. In Fig. 12, each of the graphs is separated in time by $10^{-3}/G\mu$ periods. Figure 13 shows the same for a kinky loop with 16 kinks on it, and this time 64 segments were used to represent the loop. There, each of the graphs is separated by $0.5\times10^{-3}/G\mu$ periods. Finally, Fig. 14 shows the decay of structure of a loop with 32 kinks on it. Clearly, the kink angles are opened and the straight segments between the kinks are rounded as the string evolves. Also, the loop with 16 kinks is straightening faster than the one with 8 kinks, and the loop with 32 kinks is straightening even faster. Here we have shown just the beginning of the change in string shape. Once the string becomes roughly circular, it slowly shrinks in radius.

B. Kink decay times

In order to study quantitatively how quickly this kink softening occurs, we have computed the ratio of the total energy of the loop to its mean radius. Once the string trajectory has become smooth; this number should stabilize to some approximately constant number. The string then decays almost self-similarly, with a constant energy-to-radius ratio. We define the decay time to be the time required for this ratio to get halfway to its relaxation value. Figure 15 shows this ratio as a function of time for the loop in Fig. 12. From this figure, we can estimate the relaxation time for this ratio as approximately $1.1\times10^{-3}/G\mu L$. After that time, the kinks have softened to the point that they do not contribute to the energy of the loop, which has become almost circular. Looking at Fig. 16, describing the loop with 16 kinks, this number reduces to approximately $0.5\times10^{-3}/G\mu L$.

Since the only physical quantity that can set the time scale for kink decay is its size l, we suspect that the decay time should be an approximately linear function of the size of the kink, being given by

$$t(l)_{\rm decay} \sim (\Gamma_{\rm kink} G\mu)^{-1} l \ . \tag{7.1}$$

From the decay times for loops with 8, 16, and 32 kinks, we find that $\Gamma_{\rm kink}\sim 50$. Here we have made the rough estimate of the kink "size" as $(1/N)2\pi R$, where R is the radius of the loop. Since this radius is approximately

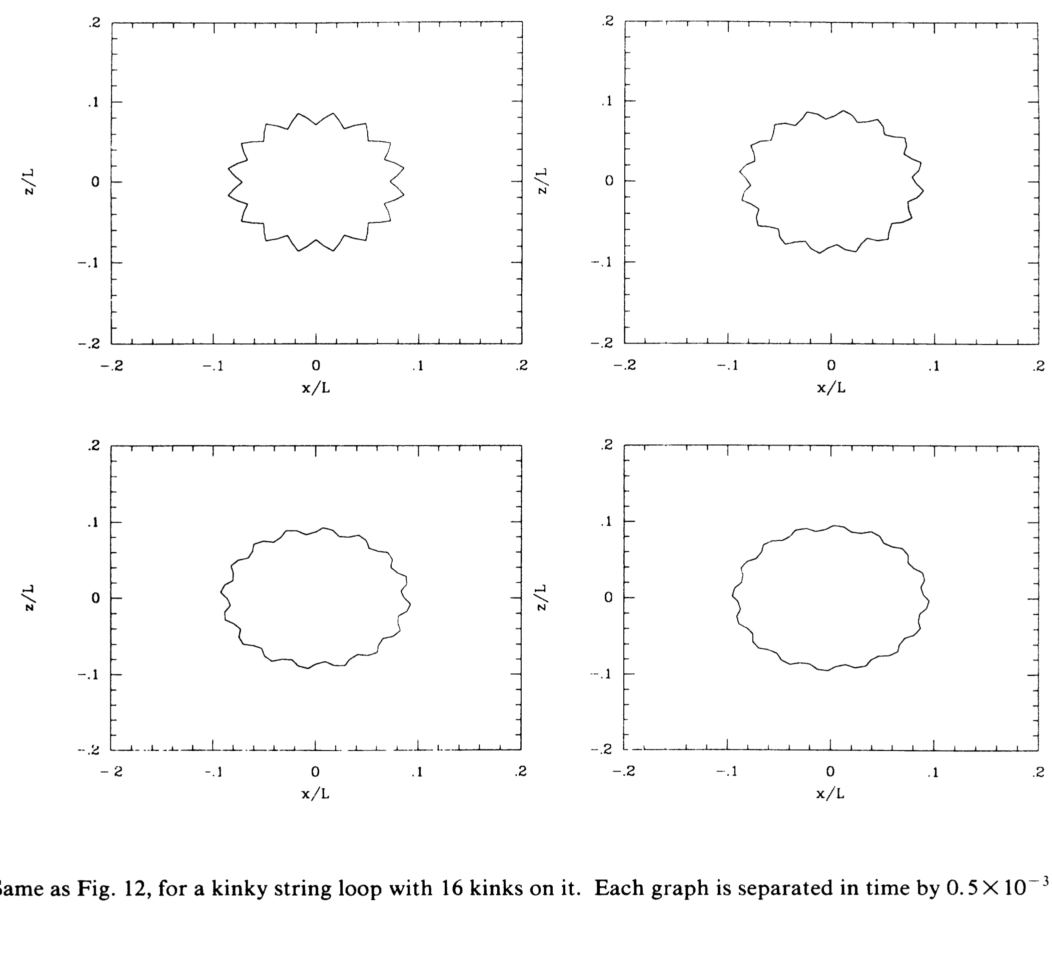

FIG. 13. Same as Fig. 12, for a kinky string loop with 16 kinks on it. Each graph is separated in time by $0.5\times10^{-3}/G\mu$ periods.

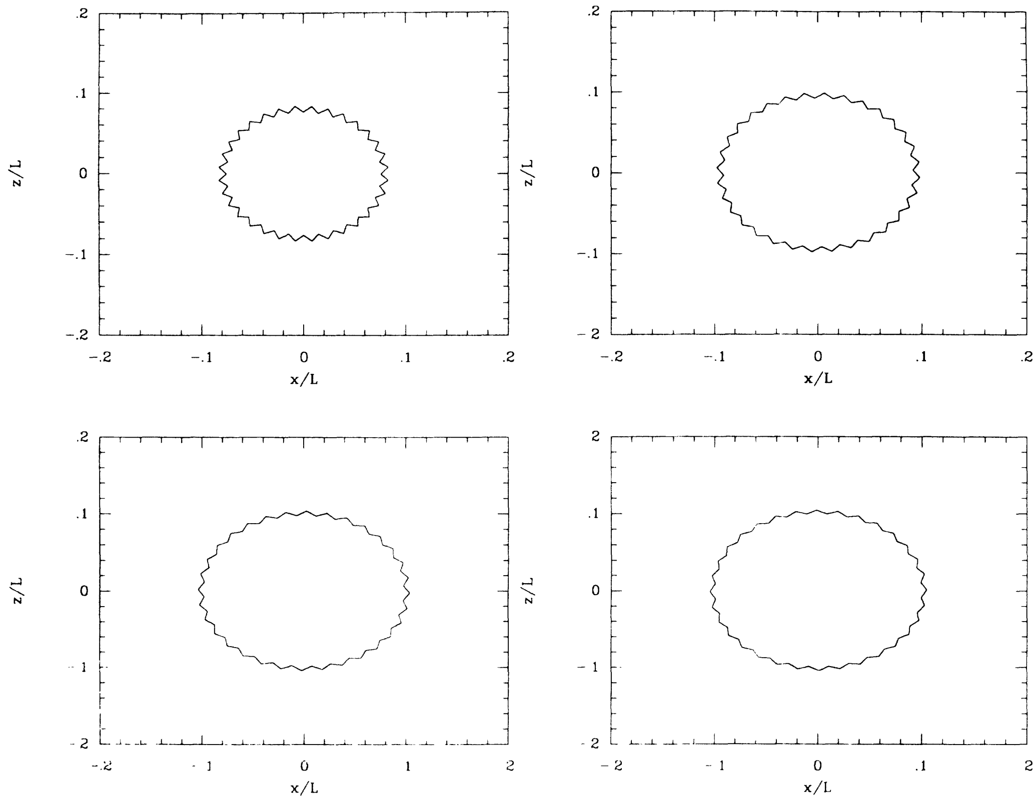

FIG. 14. Same as Fig. 12, for a kinky string loop with 32 kinks on it. Each graph is separated in time by $0.25\times10^{-3}/G\mu$ periods.

$L/4\pi$, we have estimated the kink size as $(1/N)L/2$. There is perhaps an uncertainty of a factor of 2 in the value of $\Gamma_{\rm kink}$. There is the suggestion of some dependence of $\Gamma_{\rm kink}$ on N, as well as a stronger dependence on kink opening angle. This will be investigated in a subsequent paper.

Since the gravitational back reaction is providing the smoothing mechanism, the decay time must be inversely proportional to the natural coupling constant, which is $G\mu$. Finally, that the constant of proportionality is approximately given by the gravitational power is simply a manner of energetics—the rate of loss of power in small-

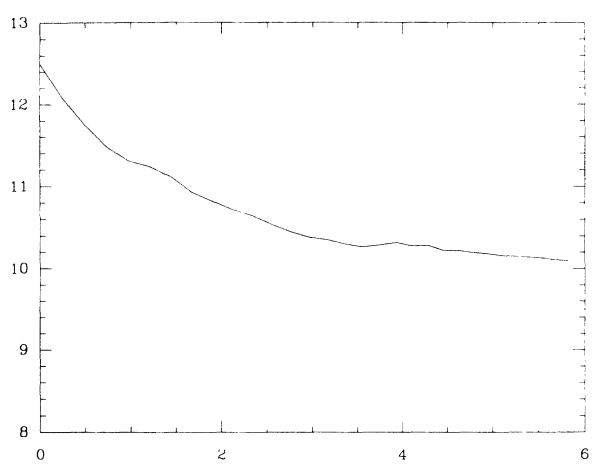

FIG. 15. Ratio of the energy to the mean radius of the loop in Fig. 12, in units of μ, as function of time (units $10^{-3}/G\mu L$).

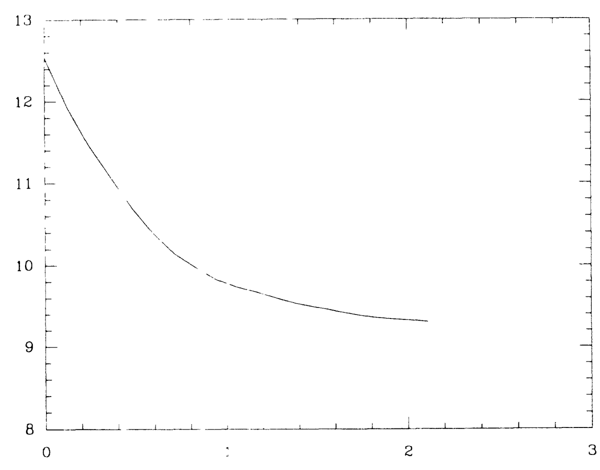

FIG. 16. Same as Fig. 15, for the loop in Fig. 12. Note the change of scale of the time axis.

scale structure on the loop is governed by $\Gamma_{\rm kink} \sim \Gamma$.

We now turn to the implications for the string scenario of galaxy formation.

C. Implications for networks and $G\mu$

In numerical simulations[6] of string evolution, long strings shrink by self-intersection (and intersecting neighboring strings). Self-intersection produces closed loops and kinks on the long strings. The loops decay to gravitational radiation. As the simulations evolve, the number of kinks per horizon along a long string grows with time. Correspondingly, the size of the daughter loops relative to the horizon size shrinks.

Gravitational radiation will limit the growth of small-scale structure on the string. The characteristic size of the loops produced at the epoch t will be on order the smallest structures on the long strings. Bennett and Bouchet argue that their simulations show that most loops produced are very small, and of size given by the small-scale "crinkly" structure on the long strings.

In the previous section, we found that the decay time kinks of scale l decays on a time of order $l/(\Gamma_{\rm kink} G\mu)$. This suggests that the characteristic loop size will scale and always be a small fraction of the horizon size:

$$l_{\rm loops} \equiv \alpha t = \Gamma_{\rm kink} G\mu t \ .$$

Since $\Gamma_{\rm kink} \simeq 50$, $\alpha \simeq 10^{-4}$ and loops will not play an important role in the formation of large-scale structure.

Loops, however, will be a significant source of gravitational radiation. The total gravitational radiation emitted by loops spawned from a string network is estimated in Ref. 6 by Bennett and Bouchet. Based on their simulations, they calculated that the energy density at a frequency ω and in a bin $d\omega$ is found to be

$$\begin{aligned} \rho_{\rm gr}(\omega) d\omega &\equiv (\Omega_g \rho_c) \frac{d\omega}{\omega} \\ &= 235 \left[\frac{G\mu}{\Gamma} \right]^{1/2} \frac{1}{\alpha} [(\alpha + \Gamma G\mu)^{3/2} - (\Gamma G\mu)^{3/2}] \\ &\quad \times \rho_{\rm rad} \frac{d\omega}{\omega} \ , \end{aligned} \tag{7.2}$$

where Ω_g is the density per logarithmic frequency interval in gravitational waves, in units of the critical closure density ρ_c, and $\rho_{\rm rad}$ is the energy density of all the radiation during the radiation-dominated era. Using $\rho_{\rm rad} = 4 \times 10^{-5} h^{-2} \rho_c$, where h is the value of the Hubble constant in units of 100 km/s Mpc, we then have

$$\Omega_g = 9.4 \times 10^{-3} G\mu \left[\frac{(\lambda+1)^{3/2} - 1}{\lambda} \right] h^{-2} \ . \tag{7.3}$$

Using our estimate for the characteristic loop size, we find

$$\Omega_g > 1.7 \times 10^{-2} (G\mu) h^{-2} \ . \tag{7.4}$$

The upper limit on the energy density in gravitational waves obtained by millisecond pulsar timing measurements[28] (95% confidence level), $\Omega_g < 4.0 \times 10^{-7} h^{-2}$, constrains $G\mu$:

$$G\mu < 2 \times 10^{-5} \ . \tag{7.5}$$

This limit still leaves plenty of room for the cosmic-string scenario of galaxy formation, which only requires a $G\mu$ of around 10^{-6}. Here there are many uncertainties, most of which are due to that in the upper limit in Ω_g. Indeed the dependence of the limit in (7.3) on λ is very weak, and we estimate that the uncertainties due to back reaction alter the limit on $G\mu$ by less than 25%. The major theoretical uncertainty is the energy density in long loops.

VIII. CONCLUSIONS

We have developed a formalism for calculating the effect of gravitational back reaction on the evolution of cosmic-string loops. We have implemented the formalism in a numerical code that can trace the evolution of a string trajectory as it shrinks due to gravitational radiation.

We have studied the long-term evolution of cosmic-string loops. The "crinkliness" of the string rapidly decays and string trajectories rapidly relax towards simple nonintersecting trajectories with typical Γ value of 50–70. These simple loops then decay in a nearly self-similar fashion. Since "crinkliness" decreases with time, gravitational back reaction does not usually lead to string self-intersections.

Cusps are not suppressed by gravitational back reaction. They are delayed, and deformed, but are still present when the back reaction is included. The back reaction does not seem to produce a string self-intersection near the cusp.

The rocket effect, the acceleration of asymmetric strings due to radiation of momentum from cusps, is suppressed by gravitational radiation. The back reaction delays the cusps and tends to symmetrize the string. Typically, the center-of-mass velocity is changed by $\Delta v \sim 0.1c$ over the lifetime of the string loop.

Kinks are straightened out by the back reaction. Typically, the decay time for a kink of size l is given by $t(l)_{\rm decay} \sim (\Gamma_{\rm kink} G\mu)^{-1} l$, where $\Gamma_{\rm kink}$ is of order 50. The decay time of the kink depends on its opening angle.

Gravitational back reaction will set the minimum scale of structures on cosmological long strings at $\Gamma_{\rm kink} G\mu$ times the horizon size. We expect that the self-intersection of long loops will produce loops of this characteristic size. These small loops are unlikely to play an important role in the formation of large-scale structure. Long strings, however, may provide seeds for the formation of sheets and galaxies.[29]

These small loops, however, are a significant source of gravitational radiation from cosmic-string loops. Using our estimates for the characteristic size of cosmic-string loops, we can recompute the expected rate of gravitational radiation: $\Omega_g h^2 = 1.7 \times 10^{-2} G\mu$. This does not include radiation from the decay of kinks along long strings.

ACKNOWLEDGMENTS

We would like to thank David Bennett, Ed Bertschinger, François Bouchet, Tsvi Piran, Bill Press, Bob Scherrer, Paul Shellard, Joe Taylor, Neil Turok, Tanmay Vachaspati, and Alexander Vilenkin for many useful comments and discussions. D.N.S. was supported in part by the A. P. Sloan Foundation and Presidential Young Investigator Program. Both J.M.Q. and D.N.S. were supported by N.S.F. Grants Nos. AST88-58145 (PYI) and PHY88-05895.

APPENDIX A

In this appendix we treat the analytical development of (3.15) and show that our formulation of the back-reaction problem is finite and well defined. We also outline how the formalism simplifies in the case of kinky strings.

We begin with Eq. (3.15), which needs to be computed and inserted into (3.14) in order to compute $\partial_u \partial_v x^\mu$, the back reaction:

$$\partial_\gamma h_{\mu\nu} = 8G\mu \int du\, dv\, F_{\mu\nu}(z(u,v)) \times \partial_\gamma[\theta(x^0 - z^0)\delta((x-z)^2)] \;, \tag{3.15}$$

where $F_{\mu\nu}$ was defined immediately following (3.13).

While the above is formally a two-dimensional integral, the retarded Green's function inside the derivative sign constrains the integration region to points on the world sheet that are earlier in time than the field point, and null relative to it. We call the curve defined by $f=0$ the *null curve,* where $f \equiv (x-z)^2$ is the Minkowski interval between field point x and source point z. Thus computing $\partial_\gamma h_{\mu\nu}$ means finding the null curve, and integrating a specified source function over it. We now develop this function from (3.15).

First, we note that we can ignore taking the derivative of the θ function. This is because that leads to a delta function $\delta(x^0 - z^0)$, which on the null curve constrains $x = z$, so that the source point collapses to the field point itself. But there, it is straightforward, to show that no contribution arises from terms $F_{\mu\nu}(x)$ in (3.15) when these are substituted into (3.14), by virtue of the gauge conditions (4.1). We may thus proceed to write

$$\partial_\gamma h_{\mu\nu} = 16G\mu \int du\, dv\, F_{\mu\nu}(z(u,v))(x_\gamma - z_\gamma)\frac{d}{df}\delta(f) \;. \tag{A1}$$

We evaluate (A1) following a discussion outlined in Ref. 9. To evaluate an integral of the type

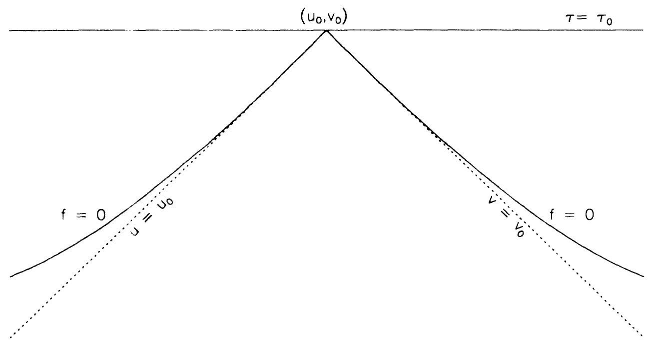

FIG. 17. Schematic drawing showing the behavior of the null curve near the field point. The null curve divides into two branches, the u and v branches, which asymptotically tend to $v = v_0$ and $u = u_0$, respectively, where u_0, v_0 are the coordinates of the field point.

$$A = \int_a^b du \int_c^d dv\, Q(u,v)\frac{d}{df}\delta(f) \;, \tag{A2}$$

we can integrate by parts. We can use the condition $f=0$ to determine implicitly either $v_{\rm ret}(u)$ or $u_{\rm ret}(v)$. Doing the former, we then have

$$A = \int_a^b du \left[\frac{Q(u,v)}{\partial_v f}\delta(f) \right] \Bigg|_{v=c}^{v=d} - \int \frac{du}{|\partial_v f|}\partial_v \left[\frac{Q(u,v)}{\partial_v f} \right]_{v=v_{\rm ret}(u)} \tag{A3}$$

We merely substitute (A1), which is of the form (A2), into (A3) in order to evaluate (3.15). The first term in (A1) is a boundary term, which is crucial when changing variables and integration region, as when going from u-v variables to σ-τ variables (e.g., the discussion in Sec. IV). Here we are interested in the short-distance behavior of (3.15); if we concentrate on the null curve near the field point, we see that it divides into two branches, which we call the u and v branches (see Fig. 17). The boundary terms for the u and v branches cancel at the field point; thus, to study the short-distance behavior of (3.15) we focus on the second term of (A3). For definiteness, we shall study the u branch. Of course, the same results (with u and v interchanged) will apply for the v branch.

Substituting (A1) into the second term of (A3), we find

$$\partial_\gamma h_{\alpha\beta} \underset{u\to 0}{\sim} -16G\mu \int \frac{du}{\partial_v f}\partial_v \left[\frac{F_{\alpha\beta}(z(u,v))(x_\gamma - z_\gamma)}{\partial_v f} \right]_{v=v_{\rm ret}(u)} . \tag{A4}$$

There are three such terms in $\partial_u \partial_v x^\mu$, from (3.14) to insert into (A4), and these must be projected out by $\partial_u x^\alpha \partial_v x^\beta$.

In particular, one must find the function $v_{\rm ret}(u)$, defined implicitly by $f=0$. Expanding the Minkowski interval $f = (z^\gamma - x^\gamma)(z^\gamma - x^\gamma)$ about the field point, and using the gauge conditions (4.1), we find

$$f \sim 2(\partial_u x^\gamma \partial_v x_\gamma)uv + \cdots \;. \tag{A5}$$

This just outlines the fact that $u=0$ or $v=0$ define the two asymptotes to which the two branches tend to. Expanding in higher orders we get

$$v_{\mathrm{ret}}(u) \underset{u \to 0}{\sim} -\frac{1}{24}\left[\frac{\partial_u x^\gamma \partial_u^3 x_\gamma}{\partial_u x^\gamma \partial_v x_\gamma}\right] u^3 . \tag{A6}$$

Using (A6) and expanding z^μ in a Taylor series about the field point x^μ, we find that contributions to $\partial_u \partial_v x^\mu$ from nearby points on the null curve are finite, going to zero as $u \to 0$ like

$$\partial_u \partial_v x^\mu \sim \frac{7}{6} G\mu \frac{\partial_u x^\alpha \partial_u^3 x_\alpha}{(\partial_u x^\alpha \partial_v x_\alpha)^2} \times (\partial_u x^\alpha \partial_v^2 x_\alpha \partial_v x^\mu - \partial_u x^\alpha \partial_v x_\alpha \partial_v^2 x^\mu) \int_u^0 du\, u . \tag{4.3}$$

We have included here only the salient points needed to derive (4.3). In essence, however, the short-distance divergence [arising from $(\partial_v f)^{-2}$ in (A4)] has been canceled by the gauge conditions (4.1) (and their derivatives).

APPENDIX B

In this appendix we show that Eq. (4.6) is equivalent to the standard expression for the gravitational power of an extended, moving body.

From Weinberg,[13] we have the following expression for the total energy radiated by an extended moving body:

$$\Delta E = 2G \int_0^\infty \omega^2 d\omega\, d\Omega [T^{*\lambda\nu}(\mathbf{k},\omega) T_{\lambda\nu}(\mathbf{k},\omega) - \tfrac{1}{2} {:}T^\lambda_\lambda(\mathbf{k},\omega){:}^2] , \tag{B1}$$

where in (B1) we take $T_{\mu\nu}(\mathbf{k},\omega)$ to be given by the Fourier transform of the real space energy-momentum tensor: namely,

$$T_{\mu\nu}(\mathbf{k},\omega) = \frac{1}{2\pi} \int d^4x\, T_{\mu\nu}(\mathbf{x},t) e^{-ik\cdot x} . \tag{B2}$$

Here the calculation is to be done on shell, since gravitational waves travel at the speed of light; hence $\omega = |\mathbf{k}|$.

We define $G_{\mu\nu} \equiv \partial_u z_\mu \partial_v z_\nu + \partial_u z_\nu \partial_v z_\mu$. Substituting (3.12) into (B1), and noting that $\int_0^\infty \omega^2 d\omega\, d\Omega$ can be written as $\int d^4k\, \delta(k^2) k^0 \epsilon(k^0)$, Eq. (B1) reduces to

$$\Delta E = 2\frac{G\mu^2}{(2\pi)^2} \int du\, dv \int d\tilde{u}\, d\tilde{v} (G^{\lambda\nu} \tilde{G}_{\lambda\nu} - \tfrac{1}{2} G^\lambda_\lambda \tilde{G}^\lambda_\lambda) \int d^4k\, \delta(k^2) k^0 \epsilon(k^0) e^{ik\cdot(x(u,v) - \tilde{z}(\tilde{u},\tilde{v}))} . \tag{B3}$$

From Ref. 14, the difference between retarded and advanced Green's functions, the radiation Green's function $D(x-\tilde{x})$, has the Fourier decomposition

$$D(x-\tilde{x}) = \frac{1}{2\pi} \epsilon(x^0 - \tilde{x}^0) \delta((x-\tilde{x})^2) = \frac{i}{(2\pi)^3} \int d^4k\, e^{ik\cdot(x-\tilde{x})} \delta(k^2) \epsilon(k^0) \tag{B4}$$

and so (B3) can be rewritten as

$$\Delta E = 2G\mu^2 \int du\, dv \int d\tilde{u}\, d\tilde{v} (G^{\lambda\nu} \tilde{G}_{\lambda\nu} - \tfrac{1}{2} G^\lambda_\lambda \tilde{G}^\lambda_\lambda) \partial_0 [\epsilon(x^0 - \tilde{x}^0) \delta((x-\tilde{x})^2)] . \tag{B5}$$

Now writing $\epsilon(x) \equiv [2\theta(x) - 1]$, and noting that the contribution from the -1 part of $\epsilon(x)$ vanishes because of antisymmetry, we obtain

$$\Delta E = 4G\mu^2 \int du\, dv \int d\tilde{u}\, d\tilde{v} (G^{\lambda\nu} \tilde{G}_{\lambda\nu} - \tfrac{1}{2} G^\lambda_\lambda \tilde{G}^\lambda_\lambda) \partial_0 [\theta(x^0 - \tilde{x}^0) \delta((x-\tilde{x})^2)] . \tag{B6}$$

In terms of $F_{\alpha\beta}$, defined immediately after Eq. (3.13) (which differs from $G_{\alpha\beta}$ only because of its third term), it is straightforward to show that (B6) is equivalent to

$$\Delta E = 8G\mu^2 \int du\, dv\, \partial_u x^\alpha \partial_v x^\beta \int d\tilde{u}\, d\tilde{v}\, \tilde{F}_{\alpha\beta} \partial_0 [\theta(x^0 - \tilde{x}^0) \delta((x-\tilde{x})^2)] . \tag{B7}$$

Now, ΔE is the energy radiated by the string. Equations (4.6) and (3.14) give the change in the energy of the string as

$$\Delta P^0 = 2\mu \int du\, dv\, \partial_u \partial_v x^0 = -\mu \int du\, dv\, \partial_u x^\alpha \partial_v x^\beta \eta^{0\gamma} (\partial_\alpha h_{\beta\gamma} + \partial_\beta h_{\alpha\gamma} - \partial_\gamma h_{\alpha\beta}) . \tag{B8}$$

The first two terms cancel because they are total derivatives (and we are integrating over a period, in u and v), and so

$$\Delta P^0 = \mu \int du\, dv\, \partial^0 h_{\alpha\beta} \partial_u x^\alpha \partial_v x^\beta . \tag{B9}$$

Finally, substituting (3.15) into (B9) we obtain

$$\Delta P^0 = -8G\mu^2 \int du\, dv\, \partial_u x^\alpha \partial_v x^\beta \int d\tilde{u}\, d\tilde{v}\, \tilde{F}_{\alpha\beta} \partial_0 [\theta(x^0 - \tilde{x}^0) \delta((x-\tilde{x})^2)] . \tag{B10}$$

Comparing (B10) with (B7) we arrive at the final result, namely,

$$\Delta P^0 = -\Delta E , \tag{B11}$$

which shows that the energy lost by the string is that radiated into space, and proves our assertion that our formulation of the back-reaction problem based on (3.14) and (3.15) is equivalent to the standard one based on (B1).

*Present address: Department of Astronomy and Astrophysics, University of Chicago, 5640 S. Ellis Ave., Chicago, IL. 60637.

[1]T. W. B. Kibble and N. Turok, Phys. Lett. **116B**, 141 (1982); N. Turok, Nucl. Phys. **B242**, 520 (1984); A. Vilenkin, Phys. Rep. **121**, 263 (1985).

[2]A. Vilenkin, Nature (London) **343**, 591 (1990).

[3]A. Albrecht, in *Symposium on the Formation and Evolution of Cosmic Strings,* edited by G. Gibbons, S. W. Hawking, and T. Vachaspati (Cambridge University Press, Cambridge, England, 1989); D. P. Bennett and F. R. Bouchet, Phys. Rev. D **41**, 2408 (1990); Princeton Reports Nos. PUPT-89-1138 and PUPT-90-1162 (unpublished); A. Albrecht and N. Turok, Princeton Report No. PUPT-90-1174 (unpublished); N. Turok, Princeton Report No. PUPT-90-1175 (unpublished).

[4]D. P. Bennett and F. R. Bouchet, Phys. Rev. Lett. **63**, 2776 (1989); B. Allen and E. P. S. Shellard, *ibid.* **64**, 119 (1990).

[5]E. P. S. Shellard, in *Cosmic Strings—The Current Status,* proceedings of the Yale Cosmic String Workshop, New Haven, Connecticut, 1988, edited by F. S. Accetta and L. M. Krauss (World Scientific, Singapore, 1989), p. 25; D. Garfinkle and T. Vachaspati, Phys. Rev. D **36**, 2229 (1987).

[6]D. P. Bennett and F. R. Bouchet, Phys. Rev. D **41**, 720 (1990).

[7]L. A. Rawley, J. H. Taylor, M. M. Davis, and D. W. Allan, Science **238**, 761 (1987).

[8]P. A. M. Dirac, Proc. R. Soc. London **A167**, 148 (1938).

[9]A. Dabholkar and J. M. Quashnock, Nucl. Phys. **B333**, 815 (1990).

[10]E. Copeland, D. Haws, and M. Hindmarsh, Phys. Rev. D **42**, 726 (1990).

[11]H. B. Nielsen and P. Olesen, Nucl. Phys. **B61**, 45 (1973); P. Goddard, J. Goldstone, C. Rebbi, and C. B. Thorn, *ibid.* **B56**, 109 (1973); J. Scherk, Rev. Mod. Phys. **47**, 123 (1975).

[12]N. Turok, Nucl. Phys. **B242**, 520 (1984); T. Vachaspati, *ibid.* **B277**, 593 (1986).

[13]S. Weinberg, *Gravitation and Cosmology: Principles and Applications of the General Theory of Relativity* (Wiley, New York, 1972).

[14]C. Itzykson and J.-B. Zuber, *Quantum Field Theory* (McGraw-Hill, New York, 1980), pp. 52 and 53.

[15]N. Turok, Phys. Lett. **123B**, 387 (1983).

[16]T. Vachaspati and A. Vilenkin, Phys. Rev. D **31**, 3052 (1985).

[17]I. H. Redmount and M. J. Rees, Comm. Astrophys. (to be published).

[18]R. J. Scherrer, J. M. Quashnock, D. N. Spergel, and W. H. Press, Phys. Rev. D **42**, 1908 (1990).

[19]R. J. Scherrer and W. H. Press, Phys. Rev. D **39**, 371 (1989).

[20]D. N. Spergel, W. H. Press, and R. J. Scherrer, Phys. Rev. D **39**, 379 (1989).

[21]C. J. Burden, Phys. Lett. **164B**, 277 (1985).

[22]W. H. Press, B. P. Flannery, S. A. Teukolsky, and W. T. Vetterling, *Numerical Recipes: The Art of Scientific Computing* (Cambridge University Press, Cambridge, England, 1986).

[23]J. M. Quashnock and D. N. Spergel, in *Cosmic Strings—The Current Status* (Ref. 5), p. 165.

[24]C. Thompson, Phys. Rev. D **37**, 283 (1988).

[25]C. J. Hogan and M. J. Rees, Nature (London) **311**, 109 (1984); T. Vachaspati and A. Vilenkin, Phys. Rev. D **31**, 3052 (1985); R. Durrer, Nucl. Phys. B (to be published).

[26]C. J. Hogan, Nature (London) **326**, 853 (1987).

[27]W. H. Press, B. S. Ryden, and D. N. Spergel, Astrophys. J. **347**, 590 (1989).

[28]D. R. Stinebring, M. F. Ryba, J. H. Taylor, and R. W. Romani, Phys. Rev. Lett. **65**, 285 (1990).

[29]T. Vachaspati, Phys. Rev. Lett. **57**, 1655 (1986); A. Stebbins, S. Veeraghavan, R. Brandenberger, J. Silk, and N. Turok, Astrophys. J. **322**, 1 (1987).